

# A Patchwork Inverse Method in Combination With the Activation Time Gradient to Detect Regions of Slow Conduction in Sinus Rhythm

Oumayma Bouhamama<sup>1,2,3</sup>, Mark Potse<sup>1,2,3</sup>, Rémi Dubois<sup>3,4,5</sup>, Lisl Weynans<sup>1,2,3</sup>, Laura Bear<sup>3,4,5</sup>

<sup>1</sup> Université de Bordeaux, IMB, UMR5251, Bordeaux, France

<sup>2</sup> CARMEN team, Inria Bordeaux – Sud-Ouest, Bordeaux, France

<sup>3</sup> IHU-Liryc, Fondation Bordeaux Université, Bordeaux, France

<sup>4</sup> INSERM, CRCTB, U1045, Bordeaux, France

<sup>5</sup> Université de Bordeaux, CRCTB, U1045, Bordeaux, France

## Abstract

*Noninvasive electrocardiographic imaging (ECGI) methods are known to produce artificial lines of block in healthy tissue. However, it remains unclear if ECGI can detect regions of slow conduction in damaged hearts. The aim of this study was to develop and test a method to detect the presence of slow conduction zones using ECGI.*

*Activation times were estimated from simulated electrocardiograms using two classical ECGI methods and a new method called the Patchwork Method (PM), which locally selects the optimal ECGI method. Five different methods (maximum, minimum, mean, nearest neighbor and random) to compute activation time gradients were then tested to pinpoint the slow conduction zones.*

*Overall, the local maximum and mean gradients both accurately located the zones of tissue damage. While the classical ECGI methods did not identify any of these regions, the Patchwork Method succeeded in identifying 5 of the 6 slow conduction zones. This novel approach thus overcomes some of the limitations of classic ECGI methods to detect regions of slow conduction.*

## 1. Introduction

Electrocardiographic imaging (ECGI) is a tool for non-invasive epicardial electrical mapping using densely sampled body surface potentials. ECGI is mathematically represented by a Cauchy problem for the Laplace equation:

$$\begin{cases} \operatorname{div}(\sigma \nabla u) = 0 & \text{in the torso volume,} \\ u = u_T \text{ and } \sigma \nabla u \cdot n = 0 & \text{on the torso surface } T, \end{cases} \quad (1)$$

where  $u$  is the electric potential and  $\sigma$  the conductivity. Several numerical methods are commonly used to solve this equation, including the finite-element method (FEM), the boundary-element method (BEM) and the method of fundamental solutions (MFS) [1].

ECGI has successfully been used to provide electro-anatomic mapping of arrhythmogenic substrates [2] and detect responders to cardiac resynchronization therapy [3]. However, recent validation studies have demonstrated that current implementations may detect artificial lines of block that are not seen in contact electrograms [4–6]. This raises the question whether ECGI can detect and locate slow conduction zones when they are present. One of the reasons this has not been evaluated is that there is no standardized quantitative method to localize regions of slowed conduction with ECGI. Instead, a purely visual approach is often used to detect isochrone crowding in activation maps.

The objective of this study was to develop a method to locate the regions of slowed conduction with ECGI and to use this method to evaluate the ability of both classic ECGI methods and a new Patchwork Method (PM) [7], to detect these areas.

## 2. Methods

### 2.1. Patchwork method

The PM locally selects the optimal solution among several classic ECGI methods. The linear relationship between the cardiac sources and the torso surface potentials after discretization can be written in matrix form:

$$Au_h = u_T,$$

where  $A$  is the transfer matrix,  $u_T$  represents the unknown cardiac sources, and  $u_T$  the torso measurements. We denote by  $A_F$ ,  $A_B$  and  $A_M$  the transfer matrices obtained with the FEM, BEM and MFS respectively.

Let  $u^{\text{ex}}$  be an array representing the exact solution of the inverse problem discretized on an epicardial mesh. Then for all methods the residual of  $u^{\text{ex}}$  tends to zero when the mesh size tends to zero:

$$\lim_{h \rightarrow 0} R_\gamma(u^{\text{ex}}) = 0, \quad \gamma = F, B, M,$$

where the residual  $R_\gamma(u_h) = A_\gamma u_h - u_T$ . The PM uses this property as a criterion to select locally, among several numerical solutions obtained with different algorithms, the one that is closest to the exact solution, without knowing what the exact solution is.

In this study, the PM solution is obtained with the FEM and the MFS and a zero-order Tikhonov regularization. For each time step  $n$ :

- The approximate solutions  $u_{h,F}^n$  and  $u_{h,M}^n$  are computed
- These solutions are used to compute the forward solution and the associated residuals  $R_B(u_{h,F}^n)$  and  $R_B(u_{h,M}^n)$  using a BEM formulation,
- For each epicardial point, a coefficient  $\alpha^n$  is defined. Its value is 0 if the smallest residual on the nearest torso point is obtained with the MFS, and 1 otherwise.

A temporal regularization of the coefficient  $\alpha$  is performed to avoid sudden variations between successive time steps. For each time step  $n$ , the new approximate solution is

$$u_h^n = \alpha^n u_{h,F}^n + (1 - \alpha^n) u_{h,M}^n.$$

## 2.2. Activation Time Gradient

An activation time gradient was used to locate regions of tissue damage, with large gradient values corresponding to slow conduction zones. The gradient was calculated for each node  $i$ , by computing the absolute difference in activation time between the current node  $i$  and the nearest neighboring nodes, defined as those within a 10 mm Euclidean distance. In order to define a single gradient value for each node, five different methods were evaluated:

- Max gradient: the maximum difference in activation time between the node and its neighbors.
- Min gradient: the minimum difference in activation time between the node and its neighbors.
- Mean gradient: the average of the activation time differences between the node and its neighbors.
- Near gradient: the difference in activation time with only the nearest neighbor.
- Rand gradient: the difference in activation time with a neighbor chosen at random.

## 3. Data

The methods used in this study were evaluated using data generated with a detailed heart-torso model that was previously tailored to a patient. We used a set of 8 simulations, including 7 with tissue damage. Activation was simulated with a monodomain reaction-diffusion equation using the TNNP membrane model [8], at 0.2-mm resolution. Extracellular potentials were computed by solving the elliptic bidomain equation in a whole-torso model at 1-mm resolution [9]. Damage patterns consisted of sheets of connective tissue aligned with the 3 coordinate axes [10].

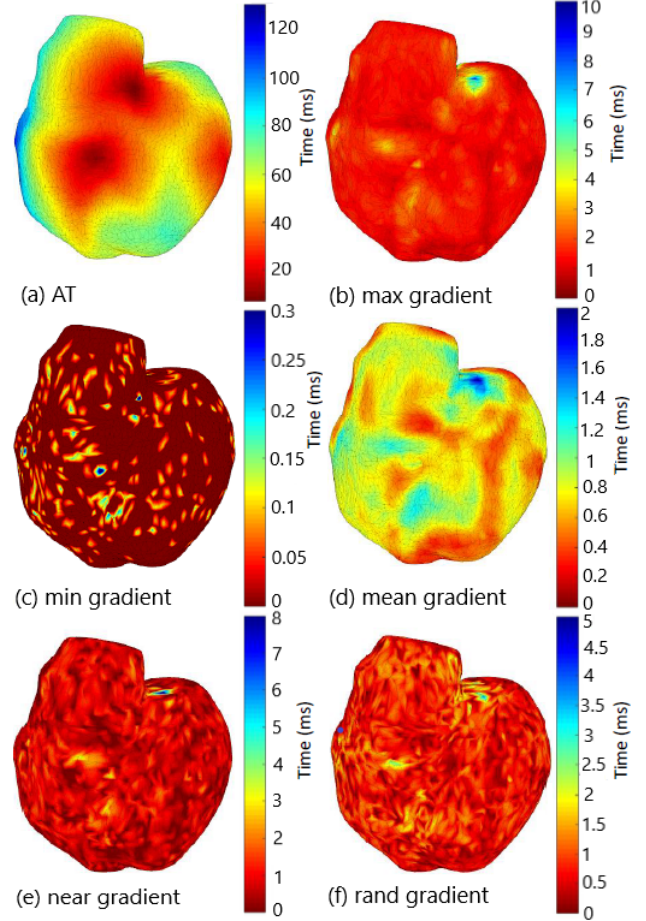


Figure 1: Recorded activation time (a) and gradient maps (b–f) calculated with different methods in a case with no tissue damage. The ventricles are shown in a 45° left anterior oblique view. The visible surface is located 3 mm outside the epicardium and the valves.

The sheets were 0.4 mm thick and were placed at 1-mm intervals. 20% of the surface of the sheets consisted of randomly placed holes. The sheets extended through the entire myocardium but not through the thin layer that represents the Purkinje system in the model.

## 4. Results and discussion

Figure 1 presents the activation time map, determined using a spatio-temporal algorithm [11], and gradient maps computed from the true (simulated) electrograms with the five different methods (max, min, mean, nearest neighbor and random) in the case with no tissue damage. A small area with large gradient value was detected at the base of the LV with all of the gradient methods. Electrograms in this area were fractionated because they originated from

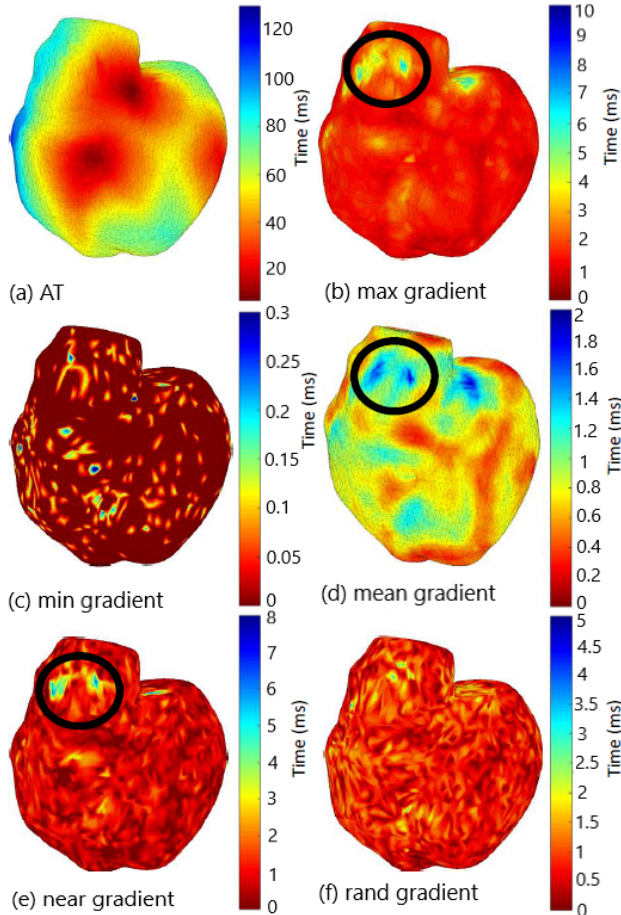


Figure 2: Recorded activation time and gradient maps calculated with different methods in one case with a damaged zone indicated by a black circle. The view is the same as in figure 1.

two disjoint muscle masses (LV and RV outflow tract). Hence the detection of the gradient is false in this area. Aside from this area, no other zone was detected, as expected in this case of no damage.

Figure 2 shows activation time and gradient maps computed from the simulated electrograms with the five different methods in one case of tissue damage. The max, mean and near gradient methods succeeded in detecting the damaged area (surrounded by the black circle) more clearly than the other methods. Moreover no other areas were detected far from the damaged areas. For the min and rand methods, the maps are irregular and do not display any informative pattern. The max and mean methods for computing the activation time gradient detected 6 of the 7 damaged regions, the near method detected only one and the min and rand method none of the damaged regions. For this reason in the following analysis we will use only the max and mean gradient methods. The only unde-

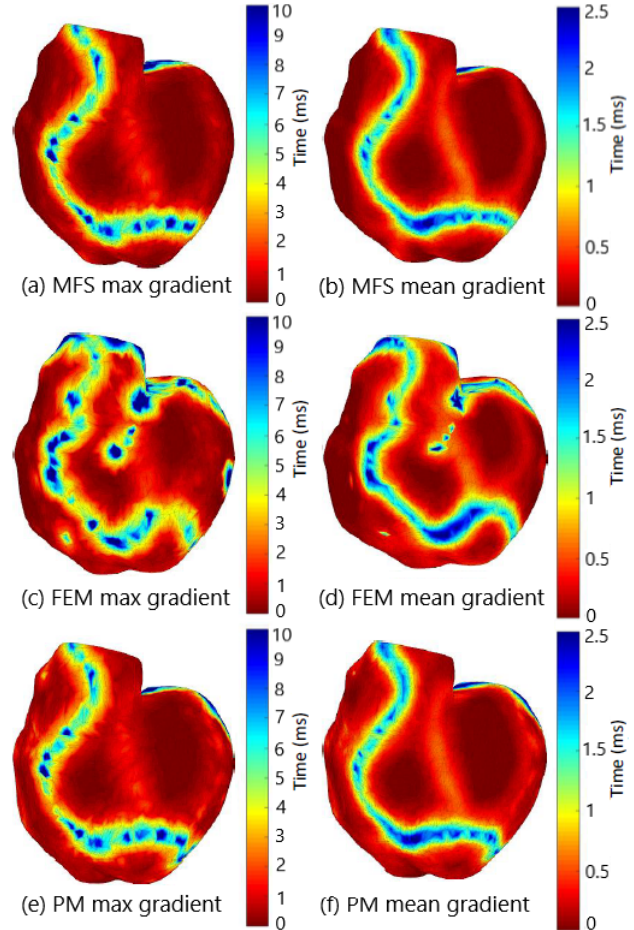


Figure 3: Reconstructed (MFS, FEM and PM) gradient maps calculated with the max and mean methods in the case of no tissue damage.

tected damaged region was located on a breakthrough site. As such, activation was not delayed inter-node but rather transmurally and an activation time gradient could not be used to locate it.

Figure 3 shows ECGI reconstructed gradient maps computed with the max and mean methods in the case of no tissue damage. Both gradient maps demonstrate artificial lines of strong gradient which surround the breakthrough sites. By analyzing the reconstructed electrograms, it can be seen that this anomaly arises due to an inaccuracy in the reconstruction of electrograms. That is, electrograms have a “W” shape during the QRS so that small changes in the voltage can cause the activation marker to jump quickly between the two downslopes and produce this artificial line. Previous studies have also seen this phenomenon [12] and suspect the appearance of W-shaped electrograms results from the reconstructed potentials representing a distant field of both the epicardial and endocardial electrical

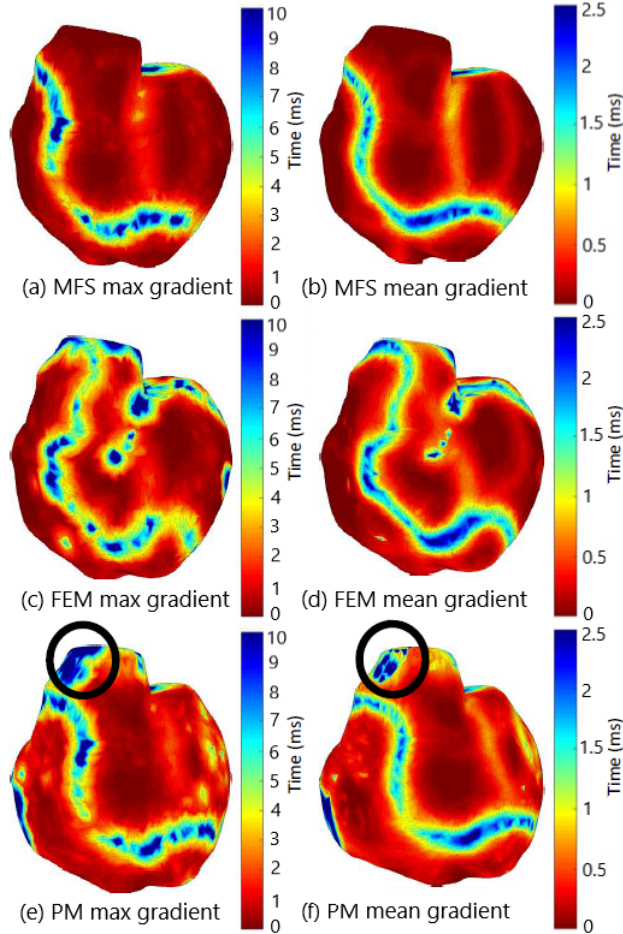


Figure 4: Reconstructed (MFS, FEM and PM) gradient maps calculated with the max and mean methods in a case of tissue damage in the zone indicated by the black circles. Same view as in the other figures.

activity and not a purely local epicardial activation.

Other than these artificial lines of gradient, no other zone of slow conduction was detected by the MFS or PM, as expected in this case of no damage. For the FEM, an extra region near the breakthrough sites was also detected in all maps.

Figure 4 presents ECGI reconstructed gradient maps calculated with the max and mean methods in one case of tissue damage. Here, the PM is the only method to successfully locate the slow conduction zone, encircled in black, with both methods of gradient calculation.

Overall, the PM method succeeded in locating 5 of the 6 slow conduction zones recorded, while the MFS and FEM reconstructions did not locate any damaged zones.

## 5. Conclusion

By computing the mean or max activation time gradient we can accurately detect regions of slowed conduction us-

ing ECGI. In particular, the novel patchwork method we proposed is an efficient tool to help overcome some of the restrictions of current numerical methods, demonstrating its abilities in detecting slowed conduction zones.

## Acknowledgments

This work was supported by the French National Research Agency (ANR-10-IAHU04-LIRYC). This work was granted access to HPC resources of CINES under GENCI allocation 2020-A0070307379.

## References

- [1] Y. Wang et al. Application of the method of fundamental solutions to potential-based inverse electrocardiography. *Ann. Biomed. Eng.*, 34:1272–1288, 08 2006.
- [2] M. Haissaguerre et al. Driver domains in persistent atrial fibrillation. *Circulation*, 8:130–530, 2014.
- [3] S. Ploux et al. Noninvasive electrocardiographic mapping to improve patient selection for cardiac resynchronization therapy. *J. Am. Coll. Cardiol.*, 61:2435–43, 2013.
- [4] L. Bear et al. Cardiac electrical dyssynchrony is accurately detected by noninvasive electrocardiographic imaging. *Heart Rhythm*, 15:1058–1069, 2018.
- [5] J. Duchateau et al. Performance and limitations of noninvasive cardiac activation mapping. *Heart Rhythm*, 16:435–442, 2018.
- [6] M. Schaufelberger et al. Comparison of activation times estimation for potential-based ECG imaging. In *Comp. in Cardiol.*, 2019.
- [7] O. Bouhamama et al. A patchwork method to improve the performance of the current ECGI methods for sinus rhythm. In *VPH Conference*, 2020.
- [8] K. H. W. J. ten Tusscher et al. A model for human ventricular tissue. *Am. J. Physiol. Heart Circ. Physiol.*, 286:H1573–H1589, 2004.
- [9] M. Potse. Scalable and accurate ECG simulation for reaction-diffusion models of the human heart. *Front. Physiol.*, 9:370, 2018.
- [10] M.G. Hoogendijk et al. Mechanism of right precordial ST-segment elevation in structural heart disease: Excitation failure by current-to-load mismatch. *Heart Rhythm*, 7:238–248, 2010.
- [11] J. Duchateau et al. Spatially coherent activation maps for electrocardiographic imaging. *IEEE Trans. Biomed. Eng.*, 64:1–8, 2016.
- [12] L. Bear et al. Advantages and pitfalls of noninvasive electrocardiographic imaging. *J. Electrocardiol.*, 57:15–20, 2019.

Address for correspondence:

Oumayma Bouhamama  
Inria Bordeaux – Sud-Ouest

